

Pairfield Fluctuations of the 2D Hubbard Model

T. A. Maier¹ and D. J. Scalapino²

¹*Computational Sciences and Engineering Division,
Oak Ridge National Laboratory, Oak Ridge, Tennessee 37831-6164, USA*

²*Department of Physics, University of California, Santa Barbara, CA 93106-9530, USA*
(Dated: October 25, 2018)

At temperatures above the superconducting transition temperature the pairfield susceptibility provides information on the nature of the pairfield fluctuations. Here we study the d -wave pairfield susceptibility of a 2D Hubbard model for dopings which have a pseudogap (PG) and for dopings which do not. One knows that in both cases there will be a region of Kosterlitz-Thouless fluctuations as the transition at T_{KT} is approached. Above this region we find evidence for Emery-Kivelson phase fluctuations for dopings with a PG and Gaussian amplitude fluctuations for dopings without a PG.

Tunneling experiments have been used to study pairfield fluctuations in both the underdoped and overdoped cuprates [1, 2]. In these experiments the tunneling current I versus voltage V between an optimally doped YBCO ($T_c^{\text{High}} \sim 90$ K) electrode and an underdoped or overdoped ($T_c^{\text{Low}} \sim 50$ K) electrode was measured. The change in the I - V characteristic $\Delta I(V)$ with the application of a small magnetic field or under microwave irradiation, which suppress the pairfield current, gives the contribution associated with the transfer of pairs from the higher T_c electrode to the fluctuating pairfield of the lower T_c electrode. Similar phenomena are well-known in the traditional low T_c superconductors [3] where the fluctuating pairfield is well described by time-dependent Ginzberg-Landau (TDGL) theory [4] with parameters set by the lattice phonon spectrum and the Fermi liquid out of which the superconducting state emerges. In the case of the high T_c cuprates, T_c/E_F is larger, the materials are quasi two-dimensional and depending upon the doping, the superconducting phase can emerge from a pseudogap (PG) phase or a non-pseudogap phase.

Various authors [5–7] have discussed the possibility of using pair tunneling as a probe to study the differences in the pairfield fluctuations between the PG and non-PG regions. Here, after defining the pairfield susceptibility and describing the type of experiment which motivated this study, we use the dynamic cluster approximation (DCA) with a continuous time auxiliary-field quantum Monte Carlo (QMC) solver to study the pairfield fluctuations for a 2D Hubbard model with an onsite Coulomb interaction $U/t = 7$ and a next-nearest-neighbor hopping $t'/t = -0.15$ in units of the nearest-neighbor hopping amplitude t . Previous calculations have shown that in the underdoped regime this model exhibits a peak in the spin susceptibility [8, 9] and an antinodal gap in the single particle spectral weight [10, 11] characteristic of a PG. Our aim is to compare the nature of the pairfield fluctuations as the superconducting phase is approached for fillings which exhibit a PG with fillings which do not.

The dynamic d -wave pairfield susceptibility $\chi_d(\omega, T)$ is given by the Fourier transform of the pairfield response

function

$$\chi_d(t, T) = -i \left\langle \left[\Delta_d(t), \Delta_d^\dagger(0) \right] \right\rangle \theta(t) \quad (1)$$

with

$$\Delta_d^\dagger = \frac{1}{\sqrt{N}} \sum_k (\cos k_x - \cos k_y) c_{k\uparrow}^\dagger c_{k\downarrow}^\dagger \quad (2)$$

In the ladder or TDGL approximation [4]

$$\chi_d(\omega, T) \sim \frac{1}{\varepsilon(T) - i \frac{\omega}{\Gamma_0}} \quad (3)$$

with

$$\varepsilon(T) = \ln \left(\frac{T}{T_c} \right) \simeq \frac{T - T_c}{T_c} \quad (4)$$

and $\Gamma_0 = 8T_c/\pi$. As schematically illustrated in Fig. 1,

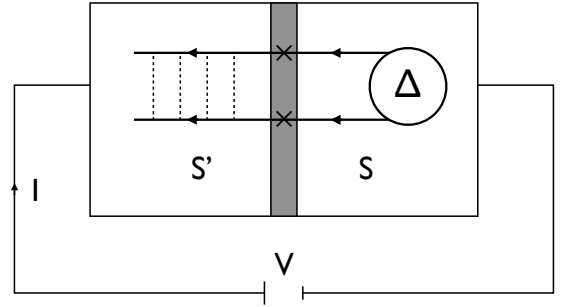


FIG. 1: Illustration of a pair tunneling experiment showing a tunnel junction separating two films S and S' . The temperature T is such that it is lower than the transition temperature T_c of the film S on the right and higher than the transition temperature T'_c of the film S' on the left. In this case there will be an excess current associated with electron pairs from S tunneling to the fluctuating pairfield of S' .

tunneling experiments [1–3] between a superconducting film S below its transition temperature and a film S' above its transition temperature find an excess current. This excess current is associated with the transfer of pairs

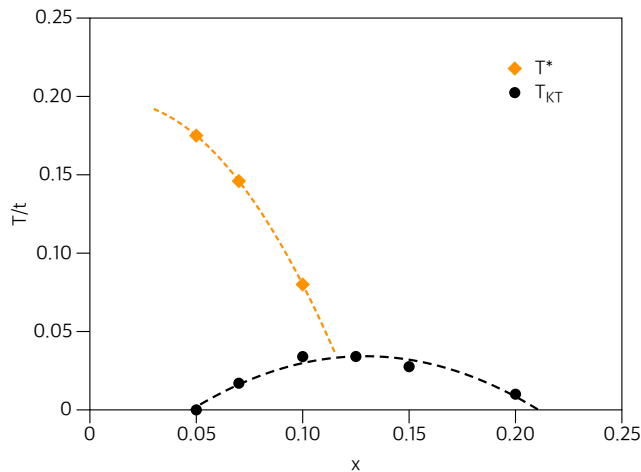


FIG. 2: (Color online) Schematic temperature-doping phase diagram of the 2D Hubbard model. There is long-range AF order at $T = 0$ for $n = 1$, a superconducting region with a Kosterlitz-Thouless [17] transition line labeled by T_{KT} and a dashed pseudogap (PG) line labeled T^* where the $q = 0$ spin susceptibility peaks. The orange diamonds mark the peaks of the spin susceptibility shown in Fig. 3, and the black circles mark the temperature at which the extrapolation of the d -wave eigenvalue $\lambda_d(T)$ reaches one.

from the superconducting side to the fluctuating pair-field on the non-superconducting side [12, 13]. This current varies as $\text{Im} \chi(\omega = 2eV)$, which for the TDGL form Eq. (3) gives

$$\Delta I(V) \sim \frac{\left(\frac{2eV}{\Gamma_0}\right)}{\varepsilon^2(T) + \left(\frac{2eV}{\Gamma_0}\right)^2}. \quad (5)$$

The temperature dependence of the peak in $\Delta I(V)$ at $2eV = \Gamma_0 \varepsilon(T)$ provides information on the nature of the pairfield fluctuations on the non-superconducting side. Independent of the TDGL approximation, in general the voltage integral of $\Delta I(V)/V$ is proportional to $\chi_d(\omega = 0, T)$.

Such experiments require a careful choice of materials and special fabrication techniques. In addition, the measurements are limited to temperatures below the T_c of the higher transition temperature film and require the careful separation of the excess pair current from the quasi-particle background. Here, motivated by these experiments, we will carry out a numerical study of the d -wave pairfield fluctuations. While this will not have the same limitations as the experiment, it is limited by our choice of the 2D Hubbard model, by the DCA approximation and by the fact that the simulation works with Matsubara frequencies. As we will see, this basic model exhibits features seen in the cuprate materials and the DCA approximation allows us to go beyond the TDGL result. In addition, we will avoid the problem of analytic continuation of the Matsubara frequencies by calculating the

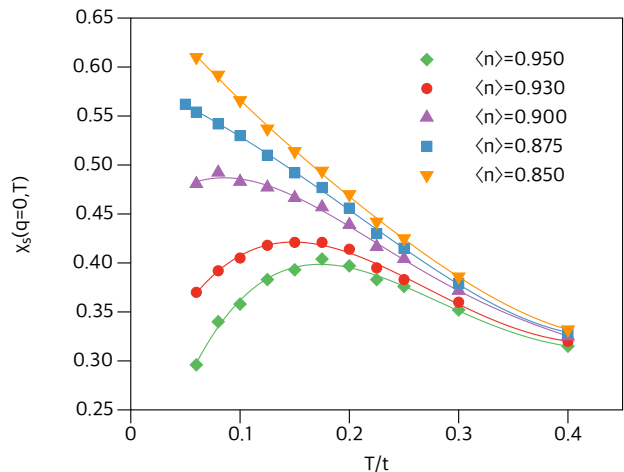


FIG. 3: (Color online) The $q = 0$ spin susceptibility $\chi_s(T)$ versus temperature for the various dopings. At the smaller dopings, $\chi_s(T)$ exhibits a peak indicating the opening of a PG.

$\omega = 0$ response, which as noted is proportional to the voltage integral of $\Delta I(V)/V$.

The d -wave pairfield susceptibility that we will study is given by

$$\chi_d(T) = \frac{\chi_{d0}(T)}{1 - \lambda_d(T)} \quad (6)$$

with

$$\chi_{d0}(T) = \frac{T}{N} \sum_k \phi_d^2(k) G(k) G(-k) \quad (7)$$

Here $G(k)$ is the dressed single particle propagator and $\lambda_d(T)$ and $\phi_d(k)$ are the d -wave eigenvalue and eigenfunction obtained from the Bethe-Salpeter equation

$$-\frac{T}{N} \sum_{k'} \Gamma_{pp}(k, k') G(k') G(-k') \phi_d(k') = \lambda_d \phi_d(k) \quad (8)$$

with Γ_{pp} the irreducible particle-particle vertex. The notation k denotes both the momentum \mathbf{k} and Fermion Matsubara frequency $\omega_n = (2n + 1)\pi T$. These quantities are evaluated using a DCA QMC approximation [14], in which the momentum space is coarse-grained to map the problem onto a finite size cluster embedded in a mean-field, which represents the lattice degrees of freedom not included on the cluster. The effective cluster problem is then solved with a continuous-time auxiliary-field QMC algorithm [15]. Here, we use a 12-site cluster (see Fig. 1 in Ref. [16]), which allows us to study the effects of non-local fluctuations, and for which the Fermion sign problem of the QMC solver is manageable down to temperatures close to the superconducting instability.

A schematic temperature-doping phase diagram estimated from these calculations is shown in Fig. 2. At half-

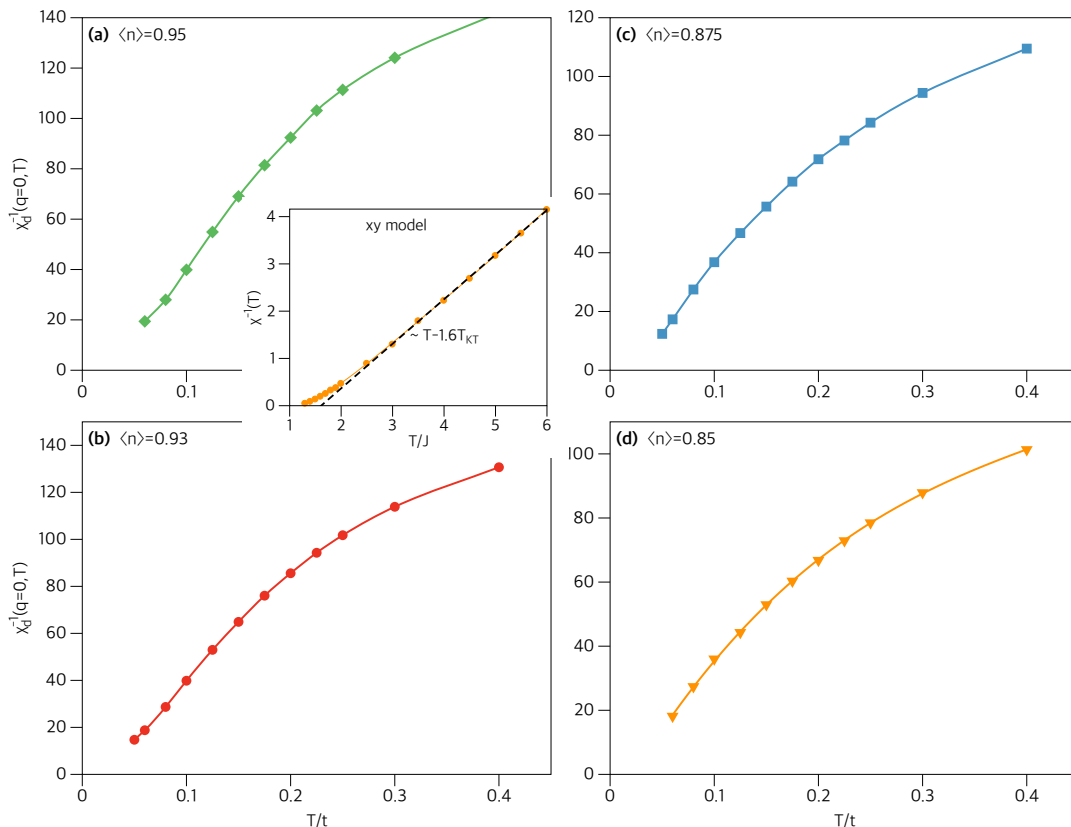


FIG. 4: Plots of $\chi_d^{-1}(T)$ for the 2D Hubbard model versus temperature for various fillings. The inset shows Monte Carlo results for the susceptibility of a 2D xy model, which has a fixed amplitude with only a phase degree of freedom that can fluctuate.

filling the groundstate has long-range AF order which is absent at finite temperature because of the continuous rotational spin symmetry. For low doping, DCA [8, 9] calculations find a peak in the $q = 0$ spin susceptibility $\chi_s(T)$. There is also evidence for the opening of an antinodal gap in the single particle spectral weight [10, 11] as the temperature drops below T^* . Results for $\chi_s(T)$ for $U/t = 7$ and $t'/t = -0.15$ are shown in Fig. 3. For $\langle n \rangle = 0.95$ and $\langle n \rangle = 0.93$ the spin susceptibility $\chi_s(T)$ peaks and then decreases below a temperature T^* which marks the opening of a pseudogap. The behavior of $\chi_s(T)$ for $\langle n \rangle = 0.875$ and 0.85 are consistent with dopings that are beyond the PG region.

At lower temperatures dynamic cluster calculations also find evidence for d -wave superconductivity [16, 18], which for a 2D system will occur at a Kosterlitz-Thouless [17] transition T_{KT} . Here we are interested in comparing the manner in which the pairfield fluctuations develop as the temperature is lowered towards T_{KT} for dopings where the superconducting phase is approached from the PG phase with dopings which do not have a PG.

If the dynamics is described by the TDGL form Eq. (3), then the peak in $\Delta I(V, T)$ will occur at a voltage which varies as $\varepsilon(T) = 1 - \lambda_d(T) \approx \chi_d^{-1}(T)$ at low temperatures. Results for $\varepsilon(T) = 1 - \lambda_d(T)$ are shown in the Supplemen-

tal Masterial. However, even if the dynamic structure of $\text{Im}\chi_d(\omega)$ is not adequately described by Eq. (3) [2, 5, 7], the voltage integral of $\Delta I(V, T)/V$ will be proportional to $\chi_d(T)$. Plots of $\chi_d^{-1}(T)$ are shown in Fig. 4 for various dopings. The inset in Fig. 4 shows Monte-Carlo results for the inverse spin susceptibility $\chi^{-1}(T)$ of the classical 2D xy model. Here one sees that there is a Curie-Weiss regime at higher temperatures associated with Emery-Kivelson phase fluctuations [19] which then crosses over to the low temperature vortex-antivortex KT behavior.

$$\chi^{-1}(T) \sim \exp\left(-\frac{b}{\sqrt{T/T_{KT} - 1}}\right) \quad (9)$$

as T_{KT} is approached.

We believe that the change in curvature of $\chi_d^{-1}(T)$ as the temperature decreases for the $\langle n \rangle = 0.95$ and 0.93 dopings reflects the onset of phase fluctuations [19] as T decreases. This behavior is analogous to that of a granular superconductor in which at higher temperatures one has a BCS $\log(T/T_c^{\text{MF}})$ behavior associated with a single grain followed by an xy Curie-Weiss behavior associated with pair phase fluctuations for a range of temperatures until the KT behavior is reached. We note that this change in curvature and the upturn at low temperatures is not seen in DCA calculations using a 4-site cluster (2×2

– plaquette). In addition, in this case, DCA calculations find that $T_c(x)$ has a maximum for $\langle n \rangle = 0.95$ and falls to zero very close to $\langle n \rangle = 1$ [20], i.e. different from the 12-site cluster results displayed in Fig. 2. We believe that this is due to the fact that (spatial) phase fluctuations and KT behavior, which reduce T_c , are absent in small clusters. This characteristic change in behavior as the cluster size is increased provides further support for the presence of phase fluctuations in the underdoped PG region of the Hubbard model.

In contrast, for $\langle n \rangle = 0.875$ and 0.85 the superconducting transition is approached from a region without a PG. In this doping regime we expect that the mean-field temperature T_c^{MF} is close to the Kosterlitz-Thouless temperature and that over most of the temperature range above a narrow region, set by the Ginzburg parameter, $\chi_d^{-1}(T)$ has the GL form $\ln(T/T_c^{MF})$. The data shown in Fig. 4(c) and (d) are consistent with this behavior.

Finally, although it is difficult to experimentally measure the large q pairfield fluctuations [2] which are necessary to determine the short distance pairfield susceptibility, in the numerical simulations this can be done. With $\Delta_{\ell+x,\ell}^\dagger = c_{\ell+x,\uparrow}^\dagger c_{\ell,\downarrow}^\dagger$ creating a pair on site ℓ and its next near neighbor site in the x direction $\ell+x$, we have calculated the local $\chi_{yx}(T)$ pairfield susceptibility

$$\chi_{yx}(T) = \frac{1}{N} \sum_{\ell} \int_0^{\beta} d\tau \langle \Delta_{\ell+y,\ell}(\tau) \Delta_{\ell+x,\ell}^\dagger(0) \rangle \quad (10)$$

This measures the local pairfield induced on the $(\ell, \ell+y)$ link when a singlet pair is created on the adjacent $(\ell, \ell+x)$ link. It's negative sign clearly shows the d -wave character of the local pairfield. We have chosen to study $\chi_{yx}(T)$ rather than the local d -wave susceptibility because $\chi_{yx}(T)$ avoids a remnant of the equal time expectation value $\langle \Delta_{\ell+x,x} \Delta_{\ell+x,\ell}^\dagger \rangle = -2\langle \mathbf{s}_{\ell+x} \cdot \mathbf{s}_{\ell} \rangle + \frac{1}{2}\langle n_{\ell+x} n_{\ell} \rangle$ which is associated with the local spin and charge correlations.

Results for $\chi_{yx}(T)$ are shown in Fig. 5. For the larger dopings, the local $\chi_{yx}(T)$ pairfield susceptibility grows as T decreases. However, for the underdoped cases, $\chi_{yx}(T)$ saturates as the temperature decreases below T^* and the system enters the PG regime. In this case the amplitude of the induced local pairfield is limited by the opening of the PG.

To conclude, the temperature dependence of the d -wave pairfield susceptibility at the larger doping is consistent with Ginzburg-Landau Gaussian amplitude fluctuations of the pairfield. At smaller dopings where the superconducting state emerges at lower temperatures from a PG phase, there is evidence that the growth of the local pairfield is limited by the opening of the PG and the increase of $\chi_d(T)$ is associated with the development of long range phase coherence.

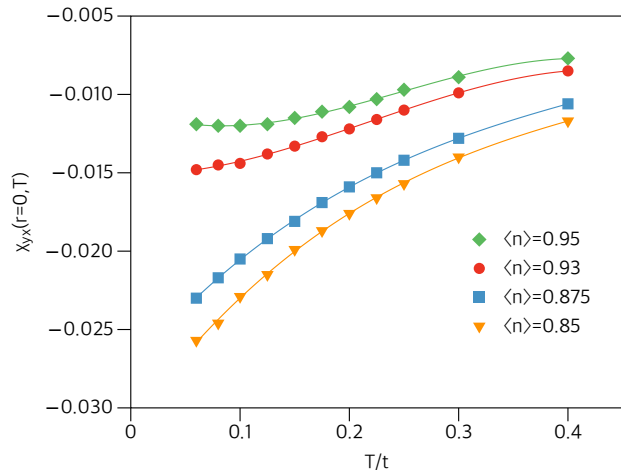


FIG. 5: (Color online) The local $\chi_{yx}(T)$ pairfield susceptibility versus temperature T for different fillings. The negative sign reflects the d -wave nature of the pairfield correlations. In the absence of a PG, these correlations continue to increase as the temperature decreases, while if there is a PG, they saturate.

Acknowledgments

The authors would like to thank E. Abrahams, I. Bozovic, I. Esterlis, M. Fisher, S. Kivelson, P.A. Lee, and A.-M. Tremblay for useful comments. We also thank I. Esterlis for the xy Monte Carlo results shown in Fig. 4 and S. Kivelson for his comment regarding the relationship of this work to granular superconducting films. This work was supported by the Scientific Discovery through Advanced Computing (SciDAC) program funded by U.S. Department of Energy, Office of Science, Advanced Scientific Computing Research and Basic Energy Sciences, Division of Materials Sciences and Engineering. An award of computer time was provided by the INCITE program. This research used resources of the Oak Ridge Leadership Computing Facility, which is a DOE Office of Science User Facility supported under Contract DE-AC05-00OR22725.

-
- [1] N. Bergeal et al., *Nature Physics*, **4**, 608 (2008). Here $\text{NdBa}_2\text{Cu}_3\text{O}_7$ provided the optimally doped electrode and $\text{YBa}_2\text{Cu}_{2.8}\text{Co}_{0.2}\text{O}_7$ the underdoped electrode.
 - [2] G. Koren and P. A. Lee, *Phys. Rev. B* **94**, 174515 (2016)
 - [3] J. T. Anderson and A. M. Goldman, *Phys. Rev. Lett.* **25**, 743 (1970)
 - [4] E. Abrahams and T. Tsuneto, *Phys. Rev.* **152**, 416 (1966)
 - [5] B. Janko et al., *Phys. Rev. Lett.* **82**, 4304 (1999)
 - [6] H.-J. Kwon, A. T. Dorsey and P. J. Hirschfield, *Phys. Rev. Lett.* **86**, 3875 (2001)
 - [7] J.-H. She et al., *Phys. Rev. B* **84**, 144527 (2011)
 - [8] T.A. Maier, P. Staar, V. Mishra, U. Chatterjee, J.C.

- Campuzano, D.J. Scalapino, *Nat. Commun.* **7**, 1875 (2016).
- [9] Xi Chen, J.P.F. LeBlanc and Emanuel Gull, *Nature Communications* **8**, 14986 (2017)
- [10] David Sénéchal, P.-L. Lavertu, M.-A. Marois, and A.-M. S. Tremblay, *Phys. Rev. Lett.* **94**, 156404 (2005)
- [11] Alexandru Macridin, Mark Jarrell, Thomas Maier, P. R. C. Kent, Eduardo D’Azevedo, *Phys. Rev. Lett.* **97**, 036401 (2006)
- [12] R. A. Ferrell, *Low Temp. Phys.* **1**, 423 (1969)
- [13] D. J. Scalapino, *Phys. Rev. Lett.* **24** 1052, (1970)
- [14] T. Maier et al., *Rev. Mod. Phys.* **77**, 1027 (2005)
- [15] E. Gull, P. Werner, O. Parcollet, and M. Troyer, *Europhys. Lett.* **82**, 57003 (2008).
- [16] T. A. Maier, M. Jarrell, T. C. Schulthess, P. R. C. Kent, and J. B. White, *Phys. Rev. Lett.* **95**, 237001 (2005).
- [17] J. M. Kosterlitz and D. J. Thouless, *J. Phys. C* **6**, 1181 (1973)
- [18] P. Staar, T. Maier, and T. C. Schulthess, *Phys. Rev. B* **89**, 195133 (2014).
- [19] V.J. Emery and S.A. Kivelson, *Nature* **374**, 434 (1995)
- [20] M. Jarrell, T. Maier, M. H. Hettler, and A. Tahvil-darzadeh, *Europhys. Lett.* **56**, 563 (2001).

Supplemental Material: Pairfield Fluctuations of the 2D Hubbard Model

T. A. Maier

*Computational Sciences and Engineering Division,
Oak Ridge National Laboratory, Oak Ridge, Tennessee 37831-6164, USA*

D. J. Scalapino

*Department of Physics, University of California,
Santa Barbara, CA 93106-9530, USA*

(Dated: October 25, 2018)

TEMPERATURE DEPENDENCE OF THE INVERSE PAIR LIFE-TIME

If the dynamics of the pairfield is described by Eq. (3), then the voltage peak $V_p(T)$ of the excess current $\Delta I(V, T)$ will be proportional to $\varepsilon(T) = 1 - \lambda_d(T)$. In this relaxation approximation, one can think of $\varepsilon(T)$ as proportional to the inverse life-time of a pair. In Fig. S1, we have plotted $\varepsilon(T)$ versus T for the various dopings discussed in this paper. Here one sees a similar behavior to the $\chi_d^{-1}(T)$ plots of Fig. 4. However, without the influence of the numerator in Eq. (6), the difference in behavior between the fillings which have a PG and those which do not becomes more evident.

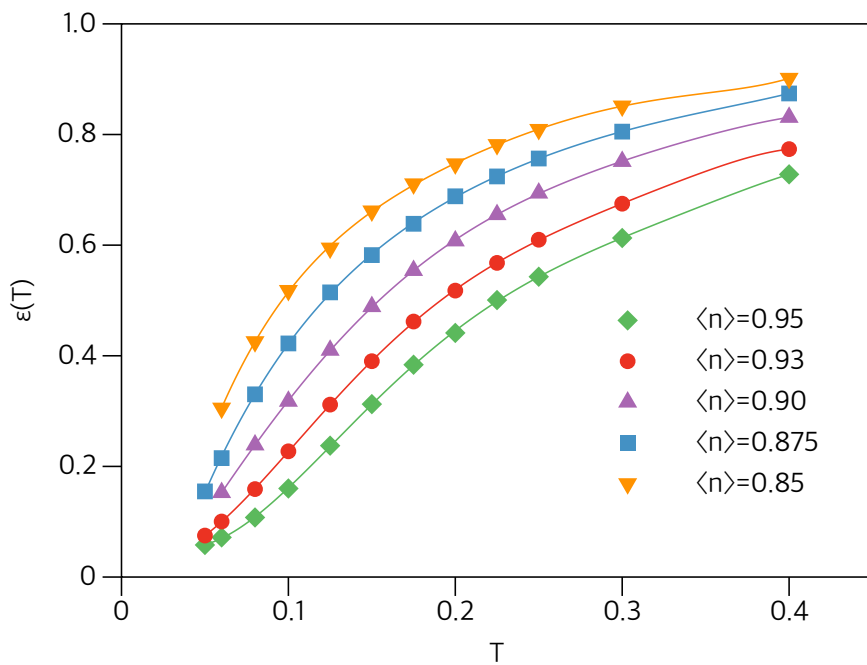


FIG. 1. (Color online) Temperature dependence of $\varepsilon(T) = 1 - \lambda_d(T)$, where $\lambda_d(T)$ is the d -wave eigenvalue of the Bethe-Salpeter equation (8) in the 2D Hubbard model, for the various dopings discussed in this paper. In the underdoped region with a PG, the change in curvature arises from phase fluctuations, which merge with KT behavior at lower temperatures, while for larger dopings, the behavior is associated with Gaussian amplitude fluctuations.

In terms of the pair life-time, one can say that for the fillings without a PG there is a range of temperatures above the KT vortex-antivortex regime, in which this time is associated with a dissociation of the quasiparticles which make up a pair. Alternatively, for fillings with a PG, the lifetime is a measure of the phase coherence time. Here, for a range of temperatures,

these can be thought of as Emery-Kivelson phase fluctuations, which, as T_{KT} is approached for this 2D system, become associated with vortex-antivortex fluctuations.